

Modeling Lithium Ion Battery Degradation in Electric Vehicles

Alan Millner

Massachusetts Institute of Technology Lincoln Laboratory, 244 Wood St., Lexington MA 02420, amillner@ll.mit.edu

Abstract -- *A new aging model for Lithium Ion batteries is proposed based on theoretical models of crack propagation. This provides an exponential dependence of aging on stress such as depth of discharge. A measure of stress is derived from arbitrary charge and discharge histories to include mixed use in vehicles or vehicle to grid operations. This aging model is combined with an empirical equivalent circuit model, to provide time and state of charge dependent charge and discharge characteristics at any rate and temperature. This choice of model results in a cycle life prediction with few parameters to be fitted to a particular cell.*

INTRODUCTION

Rechargeable lithium ion batteries offer high energy and power density and relative safety, and are therefore the battery of choice for many applications from consumer electronics to electric vehicles. Modeling the cycle and calendar life of such batteries is needed to set expectations of reliable product performance. Models to predict battery life from limited test data have fallen into two types. Models of the detailed chemistry of the cell (1), requiring extensive computation facilities, predict some time and temperature effects accurately but do not agree well with cycle life test data. Cycle life is thought to be related to precipitate formation in cracks propagating in the electrode materials of the cells, but linear relationships of cycling parameters such as depth of discharge to the resulting electrode damage have not agreed with highly nonlinear test results. Empirical models fitting test data to equivalent circuit models (2) using power law relationships fit a limited range of parameters, require extensive testing of each type of cell, and have little basis in theory. Further, such models are limited to fitting simple charge and discharge cycle data, and are not easily applied to the mixed cycle behavior of many real applications such as electric or plug in hybrid vehicles.

To address this need, the theory of crack propagation in structural materials is applied to the battery electrodes, giving a nonlinear relationship of cycling stress and temperature for use in modeling cell damage. This calculation of a damage parameter from cell history is the new part of the model, and shows a good match to available cell cycle life data. The resulting cycle life model may then be fitted to a small amount of cell test data. This life damage parameter is then applied to the empirical equivalent circuit model structure, where it is found to be a good fit to test data. Such a model is constructed in a MATLAB program capable of reading in the charge-discharge profile of either lab cell tests, or actual vehicle driving histories from hybrid electric vehicle simulations, or real vehicle data. This allows a mixture of complex battery usages to be included in lifetime predictions with limited computational requirements.

THEORY

The electrochemical modeling of lithium ion batteries and their degradation with cycling and time is described (3) in terms of several mechanisms. One is the deposition of insoluble lithium precipitates on surfaces in the carbon electrode, removing lithium from the active cell. This can progress as new surface is exposed by crack propagation or exfoliation in the MCMB or graphite structure of the anode. A second is the separation of anode or cathode material from the electrical collector metal at either electrode. Both are essentially physical crack propagation mechanisms excited by stresses and temperature over cycling and time. The second mechanism is less of a factor in modern lithium ion batteries due to the nature of their fabrication (4) with intimate contact between electrode materials. The end effect is a reduction in charge capacity and an increase in resistance. Since the damage is a single mechanism, it can be represented by a single lumped damage parameter L , varying from 0 to 1 as the cell ages from new to having no capacity left at all. This allows the model to be split into two parts, the first

being the damage calculation accumulated as the value of L due to cell history, and the second being an equivalent circuit model of the cell as a function of age L and state of charge SOC.

By convention, end of life is defined as 80% of original capacity remaining at the test discharge condition. For convenience then, it is useful to create the equivalent circuit model so that at the value L=0.2, the cell charge capacity at the C rate at T=25C is approximately 80% of its original capacity, giving some intuitive value to the parameter L. . These effects can then be represented in an equivalent circuit model as variable series resistances which are functions of the damage parameter, the state of charge, and temperature. The basic circuit model approach is described by a modified form of the Shepherd equation (1,5), which describes the battery terminal voltage and current as a sum of an open circuit voltage, a polarization resistance term dependent on state of charge, and an ohmic resistance term.

The major problem with the physical models is that they do not provide a prediction of battery cycle life that is strongly nonlinearly dependent on depth of discharge, while this dependence is seen in empirical reports of cycle life testing of lithium ion batteries and many other battery types (6, 7, 8). Because there is no driving nonlinear mechanism in prior physical models for this damage parameter as a function of depth of discharge, the resulting loss of capacity is approximately a linear function of charge throughput. In order for the physical models to address the nonlinear dependence, a mechanism is needed with a fundamentally nonlinear nature.

Crack propagation theory offers such a mechanism. Zhurkov (9) assumes crack propagation to be a thermal phenomenon, excited by an external stress added to random thermal stresses with an activation energy threshold. In explaining the crack propagation mechanism for failure of solid structures, Zhurkov shows a good fit to experimental data for structural failure with his resulting formula for material fracture time t:

$$t=t_0 * \exp[(U_0-gS)/kT] \quad (1)$$

If we rearrange this to represent a rate of propagation inversely proportional to t, then

$$t_0/t = \text{normalized rate} = \frac{\exp[(gS-U_0)/kT]}{\exp(-U_0/kT)} \quad (2)$$

The resulting rate due to the dominant first term shows aging at modest stresses (calendar life) is highest at high temperature T. This is in fact the Arrhenius relationship, and is widely utilized in battery models (3). This agrees with battery manufacturers' data (10) showing approximate doubling of degradation rate for a given

depth of discharge for every 10 degree C rise in temperature. This thermal dependence has been recognized in the literature, but often identified as part of the Tafel equation (3). It is suggested here that since such reactions may reach equilibrium until new surfaces are exposed by cracking, this dependence may be due to the crack propagation phenomenon instead.

MODELING DAMAGE

The Zhurkov formula indicates that the rate increases exponentially with the stress level S. If the stress level is related to the swing in state of charge in a cycle, this would also match the data. Taking this further, if we take the room temperature aging of the battery to be about 10 years, and we take from the data that the aging process speeds up by a factor of 2 every 10 degrees C, then we get values for some constants in the Zhurkov equation.

The details of the second term are difficult. First, we separate the effects of average state of charge (average cell voltage, the Tafel relation) from the stress effects of state of charge swing. To address the two effects, we introduce the variable SOCavg representing the average state of charge over the cycle, and the variable SOCdev representing the normalized deviation of the state of charge from its mean over a cycle period.

The dependence of degradation due to micro-cycles of depth D with an average state of charge SOCavg must cope with the effect of that average state of charge and its associated average voltage. To deal with a mixed cycle with an arbitrary SOC, we introduce the definition of SOCavg = the mean state of charge over the time interval of cycling. Let the time interval m be the mth time the car battery is discharged and recharged over a trip. One way of looking at this is the effect of the overpotential described in (1).

$$\text{SOCavg} = \int_{\text{time interval } m} \text{SOC}(t) dt \quad (3)$$

For a cycle in which the SOC is a ramp from 1.0 down to 0 and back to 1.0, the deviation in SOC is 1/2/sqrt(3). Therefore we invert this value for normalization, and define the normalized deviation as:

$$\text{SOCdev} = 2\sqrt{3} * \frac{\int_{\text{total time}} (\text{SOC}(t)-\text{SOCavg})^2 dt}{\int_{\text{total time}} dt} \quad (4)$$

Using SOCdev as a fraction of 1.0 for the latter effect, we assign a coefficient K_{co} for the exponential term.

Note that this degradation must be linear over multiple identical cycles, so we need a coefficient linear in normalized throughput charge. The time interval defining

SOCdev must include both discharge and recharge. This has the value of 1.0 for the full 100% DOD cycle, and is proportional to depth of discharge for a single smaller cycle. We must include the possibility of multiple charges and discharges in the time interval under consideration. To account for this, let Q_{nom} = the nominal charge capacity of the battery and $abs(I)$ = the absolute value of battery current at a time t . Then the effective number of throughput cycles N in the time interval is given by

$$N = \int_{\text{time interval}} \frac{abs(I(t))dt}{Q_{nom}/2} \quad (5)$$

The factor of 2 arises because we have counted both charge and discharge currents. For cycles centered on 50% SOC, we then have the increment in life parameter given by

$$Life1 = K_{co} * N * \exp((SOCdev-1) / K_{ex} * Tnabs/Ta) + 0.2 * t_{cycle}/t_{life} \quad (6)$$

Here the value of t_{life} is the estimated calendar life to 80% capacity. Equating the exponential in the new calculation to the Zhurkov term gives

$$(SOCdev-1) * Tnabs / (K_{ex} * Ta) = gS/kTa \quad (7)$$

The details of the mechanical strain from dimensional change in the carbon anode during intercalation of lithium ions in relation to cycle parameters are complex, and would depend on the specific battery, and must be taken from test data. The value of the resulting constants K_{co} and K_{ex} would be battery specific and are empirically fitted to battery life data. K_{co} would be set for 100% DOD life, and K_{ex} matching life at some lower DOD. Using Peterson's data (11) for the A123 ANR26650M1A cell, a particular cylindrical lithium iron phosphate battery intended for PHEV use, the values best fitting data for $D=0.35$ to 0.95 were found to be $K_{co}=3.66E-5$ and $K_{ex}=0.717$.

Then the degradation is adjusted to account for average state of charge, and to show the degradation rate is

proportional to the concentration of Lithium ions left in active form, using the formula

$$Life2 = Life1 * \exp(K_{soc} * (SOC_{avg}-0.5)/0.25) * (1-L) \quad (8)$$

For the Peterson A123 data, $K_{soc} = 0.916$. This parameter accounts for the effect of voltage averaged over a cycle, matching the Tafel relationship. If the battery cycle is performed starting at full charge and decreasing to a fixed DOD, then returning to full charge, then the larger the DOD the higher the SOC_{avg} . The combination of the higher degradation due to high SOC_{dev} and lower degradation due to lower SOC_{avg} can obscure the trends and confuse the analysis of data. Separation as shown here gives an excellent fit over a wide range of possible cycles.

Since the result is nonlinear in SOC_{dev} , the superposition principle may not be applied directly to state of charge variation for battery cycling at arbitrary depths of SOC, so the model for such a phenomenon over arbitrary use will be complex. However, at the end of each cycle, the state of the material is a function only of its history (it is a state variable) and for simple histories like a series of identical cycles of different amplitudes, this can be compared. Such simple repeated cycles at varying SOC_{dev} are the only lab data really available for batteries. So, if we construct a nonlinear model matching the data at high and low d cycles, such a model should yield useful results. The accuracy of the model over a broad range of parameters attests to the good fit of the basic theory behind the form of the model. To show this, the data from (6) and (11) is re-plotted in figure 1 in this fashion. The fit is excellent. More data over a wider range of parameters will allow better comparison for more battery types.

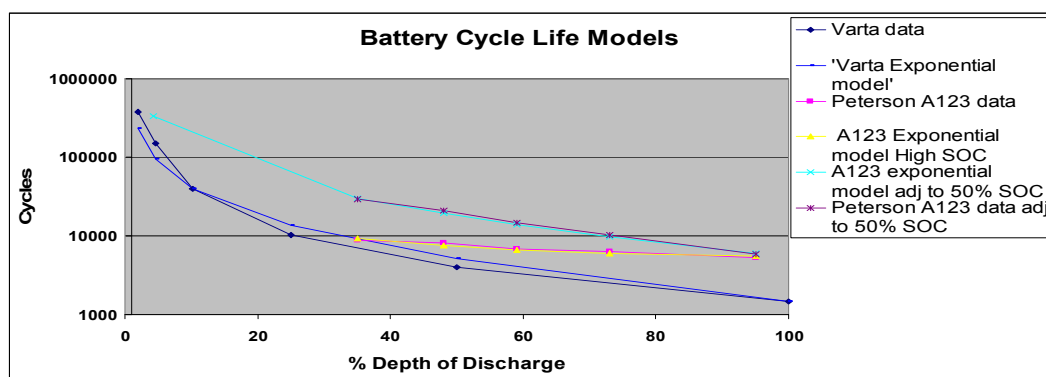


Figure 1. SOCdev vs. log cycle life for Li Ion batteries. The adjusted Peterson data is shown as it would be predicted to be at a 50% average SOC

Finally, the battery aging rate is adjusted for temperature using an Arrhenius relation as predicted by the Zhurkov model, giving the total increase in the aging parameter L for the cycle m :

$$\text{Life}(m) = \text{Life}_2 * \exp(T_{\text{fact}} * (T - T_{\text{nom}}) * (T_{\text{nabs}} / T_a)) \quad (9)$$

Where comparing with the Zhurkov formula, $T_{\text{fact}} = U_0 / k T_{\text{nabs}}^2$. The manufacturer's data (10) indicate that the value of T_{fact} is $\ln(2) / 10 = 0.0693$, giving a doubling of decay rate for each 10 degree C rise in temperature.

A rate dependence of battery life due to both charging and discharging rate is has been documented. However, for rates within the range discussed, it is not clear whether internal heating at high charge rates might account for the entire phenomenon of accelerated degradation at high rates. Other data for modern lithium ion batteries tested for cycle life over a wide range of rates and depths of discharge tends to be proprietary; there is a lack of such data in the open literature at present. It is clear that proper thermal management of the cells is needed to mitigate the effects of high rate charge and discharge. So, for this model, the cell temperature will be taken as a constant including any self-heating effects. No other rate dependent mechanism is included here.

The damage over the life of the battery for M time intervals or vehicle trips is then given by

$$L = \sum_{(m=1 \text{ to } M)} \text{Life}(m) \quad (10)$$

This variable L will change over the life of the battery from 0 (new) to 1.0 (no capacity left), and may be thought of as the fraction of lithium still active in the battery. While it is crudely related to the charge capacity left in the battery, that value must take into account the voltage limits for operation and the detailed voltage vs. time curve of the battery, given by the equivalent circuit model.

EQUIVALENT CIRCUIT MODEL

The next task is to utilize this theoretical basis for progressive damage to construct an equivalent circuit model that will predict the terminal characteristics of a lithium ion battery for any given charge and discharge profile, temperature, and rate, including partial cycles and multiple cycles, as might be encountered in driving a hybrid vehicle or utilizing it in a vehicle to grid energy exchange. Here it is necessary to restrict the class of cycles to those with rates and temperatures that do not initiate physical processes not included in the model. For

modern lithium ion batteries in vehicles, these are generally rates below $\pm 5C$ and temperatures between $-20C$ and $+45C$ (10).

To complete the equivalent circuit model given the damage parameter L , the work of Liaw (12) is used to establish the form of the result. Define the open circuit voltage of the battery including a polarization term by:

$$\begin{aligned} V_{oc} &= V_{nom} + \text{SOC} * (V_{max} - V_{nom}) / 2 \\ V &= \text{voltage} = V_{oc} + (R_1 + R_2) * I \end{aligned} \quad (11)$$

The formula for R_2 (L , SOC is adapted from (12) :

$$R_2 = a + b * (\text{SOC})^c + d * (1 - \text{SOC})^c \quad (12)$$

Here the parameters a - e are functions of the damage parameter L . The first term is mid-SOC resistance, the second low SOC resistance, and the last high SOC resistance (limiting capacity). The parameters a , b , and d have dimensions of resistance and scale with the mid-SOC internal resistance. To ratio this to the fixed resistance R_1 , we here define the dimensionless variable resistance scaling factor R_s so that the variable resistance is scaled from the reference model by a factor of $R_s * R_1$. L is the lifetime damage parameter described above.

We then have the form of the equivalent circuit model. This is fitted to the battery selected to reproduce the values of R_2 required at different points in the life L . It includes a scaling factor R_s to allow different size cells or banks of cells of the same type to be modeled easily from a basic cell of the same type, where $R_s = R_1 / R_{ref}$ is the ratio of the initial resistance of the cell bank to the reference cell. For this example cell $R_{ref} = 0.011$ ohms. This avoids needing to re-fit the coefficients to the battery cell unless its character is very different from the one modeled here. All coefficients have been adapted from (12) to give the discharge curves of (10) and be compatible with the life parameter L scaling described above:

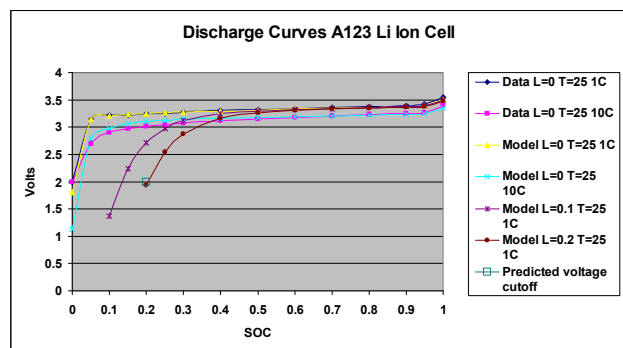


Figure 2. Discharge curves for cell model compared with manufacturer's data.

$$\begin{aligned}
 a &= R_s \cdot \text{TempcoR} \cdot (7.188e-3 \cdot L + 5e-4) & (13a-e) \\
 b &= R_s \cdot (0.0391 \cdot L + 5e-3) \\
 c &= -6.25L + 2.3 \\
 d &= R_s \cdot \text{TempcoRlo} \cdot (1.71e-3 \cdot L^3 + 6.25e-4 \cdot L^2 + 4.69e-5 \cdot L + 8.44e-9) \\
 e &= 10.828 \cdot (L + 2E-3)^{-0.0645}
 \end{aligned}$$

The form of these coefficients is relatively laborious to determine from cell test data compared to the damage model for the parameter L, so unless the actual equivalent circuit model value R2 is needed to determine capacity at different rates, the value of L=0.2 giving nominally 80% charge capacity can be used as a simpler measure of end of useful life.

For a bank of batteries with Ns cells in series and Np cells in parallel, the open circuit voltage is multiplied by Ns and the resistance of the bank R1 is scaled by Ns/Np. The thermal effect on equivalent circuit elements is simplified into the following relationships:

$$\text{If } T \geq T_{nom} \text{ then } \text{TempcoR} = \text{TempcoRlo} = 1 \quad (14a)$$

Using this model, the suitability of today's lithium ion batteries for plug-in hybrid vehicle use, with or without V2B, can be evaluated.

The model is re-run in figure 3 for the case of 50% swing in SOC, swinging from full to half charge, at the temperature of 35C. This might represent the use of the battery in a vehicle to grid mode several times a month to level peaks in the electrical power demand of the employer's facility. Note that the cycle life of 4500 cycles might represent 75 years of 5 cycles a month, a rather benign scenario. Lower temperature due to a shaded location for the vehicle or a cooler climatic location would represent an even better result.

Consider the effect of extra V2B cycling in purely dollar terms. If the battery were used for V2B at 50% DOD from full charge, T=35C, the life to 80% capacity would be about 5000 cycles. If this battery cost \$5K, the dollar cost per V2B cycle of battery replacement would be \$1. So, perhaps up to ten of these per month could easily be afforded to capture the \$100/month/car of V2B revenue without significantly aging the battery.

$$\begin{aligned}
 \text{if } (T < T_{nom}) & & (14b) \\
 \text{TempcoR} &= 1 + 10 \cdot ((T_{nom} - T) / 20)^2 \\
 \text{TempcoRlo} &= 1 + 5 \cdot ((T_{nom} - T) / 20)^2
 \end{aligned}$$

This gives a resistive equivalent circuit model for all L, SOC, and T values allowing terminal voltages and currents to be calculated and charge capacities under any desired condition to be predicted.

RESULTS

The above model is implemented in Matlab and applied to the A123 ANR26650M1A cell in a bank for a PHEV having Ns = 56, Np = 11. This is a state of the art plug-in hybrid electric vehicle battery and has been used in a large number of retrofit vehicles on the road today. The resulting discharge curves are shown in figure 2. The initial curves are a good match to the vendor's data sheet, and the aging ones discharged to 2.0 volts per cell match the capacity curves in the same reference data sheet.

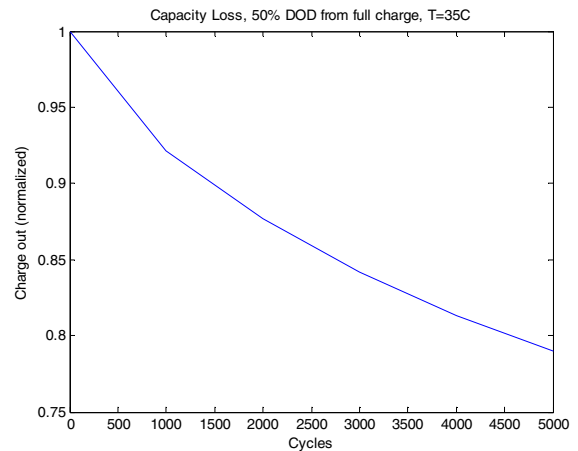


Figure 3. Capacity loss in simulated cell using exponential model, 75% average SOC, 50% swing in SOC, T=35C, tested at C rate.

On the other hand, a 100% deep discharge cycle at 45C with no micro-cycling, shown in figure 4, would reduce the battery to 80% capacity within 1700 cycles (4.6 years of commutes or \$1.00 per V2B cycle), so these deep cycles at high temperature are to be avoided. Smith (13) points out the need for thermal management of such batteries in parked vehicles in hot climates. Keeping battery temperatures below 35C by avoiding peaks in temperature appears feasible and beneficial. Limiting depth of discharge for V2B also appears to be a good choice to avoid reducing battery life.

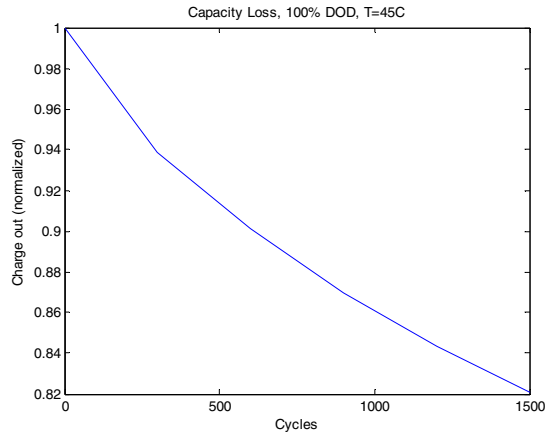


Figure 4. Capacity reduction with 100% DOD cycles at a temperature of 45C.

The simulated battery bank is then exposed to aging due to micro-cycles similar to those often estimated in driving a typical PHEV, and at intervals the capacity is measured by test discharging the simulated cell using the equivalent circuit model. Figure 5 shows the charge capacity reduction with age in micro-cycles for a temperature of 35C and a discharge rate of 1C. Note that with over 200 thousand micro-cycles of life, if commuting equated to 25 micro-cycles per day this represents over 20 years of use, more than adequate life. So it is the deep cycles of driving, not the micro-cycles, that will probably dominate the aging of the battery. Also note that at 45C, half this life would barely be adequate. Note also that the average SOC should be kept low to minimize aging effects.

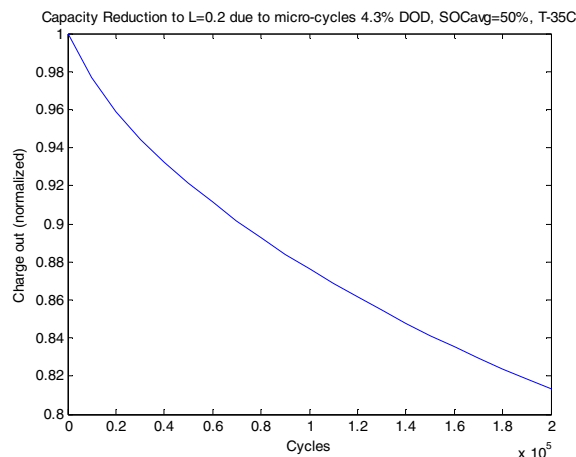


Figure 5. Capacity loss in Lithium Iron Phosphate cell, exponential battery model, micro-cycle SOC swing = 4.34%, average SOC = 50%, T=35C, tested at C rate.

The model is then applied to a simulated vehicle commuting profile putting both the long overall discharge and the micro-cycling combined. This simulation uses the vehicle characteristics of a Toyota Prius with a 5kWh

plug-in hybrid (about a 10 mile electric range). The basic cycles of vehicular use consist of the long term depletion of the battery each trip, overlaid with the micro-cycle effects of driving. The plot of state of charge vs. time for a 24 mile commute based on the aggressively driven US06 route repeated 3 times is shown in Figure 6. When actual vehicle performance files are made available, the model will accept those as well.

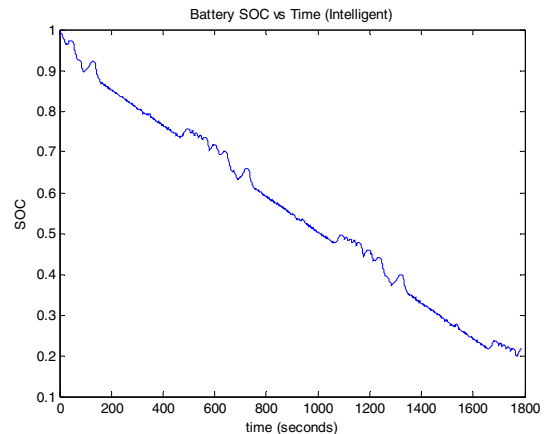


Figure 6. State of charge vs. time for a 24 mile US06 commute with predictive energy control.

In this case the battery was allowed to discharge from 100% to 20% SOC (a very deep cycle for such a car) while a controller maintained the SOC along an approximately linear SOC trajectory over the trip to maximize gasoline efficiency. Such a trip at a maximum temperature of 45C is calculated by the model to use $2.55e-4$ of life per trip. It would use up 20% of the life of the battery in only 814 trips (2.2 years of daily trips) at this rate; clearly not adequate life.

However, if the battery temperature were reduced to 35C by using a battery thermal management system, and the discharge limited to a 60% swing between 90% and 30% SOC (which would burn more gasoline), then the battery life would be 2732 trips, or 7.5 years with daily trips. This battery management is more typical of today's plug-in hybrids. This would be only marginally adequate, showing that life in PHEVs is barely meeting expectations with today's batteries, and indicates the cycle life improvements needed.

CONCLUSIONS

The aging effects of cycling at arbitrary depths of discharge, average states of charge, temperatures and combined uses can be evaluated using a new model. The approach focuses on crack propagation as the dominant mechanism of degradation, and uses an exponential

dependence of ion loss on stresses such as depth of discharge, average state of charge, and temperature, consistent with crack propagation theory. The model to this point requires a small number of cell measurements. The resulting life parameter is a measure of ion concentration as a function of cycle life. The calculation of this aging parameter and its relationship to a life defined as 80% capacity allows evaluation of different uses and charge control strategies.

Beyond this, an equivalent circuit model of the battery cell or bank is constructed to provide terminal characteristics as a function of time, age, state of charge, and charge or discharge rate. This allows calculation of charge capacity under any desired rate and temperature condition with any desired discharge termination voltage.

The model is then exercised for a current state of the art lithium iron phosphate battery being used in plug-in hybrid electric vehicles, using varying deep cycles at varying average state of charge, using micro-cycling at varying average state of charge, and using actual discharge time profiles from simulated vehicle operation.

The results show that the battery life can be maintained in an acceptable range for PHEV use if very deep cycles (<60%DOD) are avoided, if temperatures are kept low (<35C), and if average state of charge is kept low (<60%). Vehicle to grid operation of a few cycles per month has negligible effect compared to driving if these same guidelines are applied. These parameters represent the areas of needed improvements in the state of the battery art for future developments, and the model provides a means of quantitatively evaluating such advances.

Notation:

DOD = depth of discharge, 0 to 1.0
 g = a coefficient representing anharmonicity for a given crystal lattice
 I = current, Amperes, positive = charging
 k = the Boltzman constant = $1.38 \cdot 10^{-23}$ J/degC
 K_{co} , K_{ex} , K_{soc} = constants in model equation, respectively the coefficient of throughput, the exponent for depth of discharge, and the coefficient for average state of charge.
 Ns = number of series cells in a bank
 Np = number of parallel cells in a bank
 Life1 = increment of life parameter in a cycle accounting for swing in SOC and throughput
 Life2 = increment of life parameter accounting for average SOC and decrease in lithium ion concentration
 Life (m) = increment of life parameter L including thermal effects for cycle m
 L = life aging parameter from 0 to 1.0

R1 = the equivalent fixed resistance of the battery bank, new
 R2 = the variable resistance of the battery, a function of L and SOC
 S = stress applied
 SOC = state of charge, 0 to 1.0
 SOCavg = average state of charge over a cycle
 SOCdev = deviation in state of charge in a given cycle m
 t = time in seconds
 t0 = the period of atomic oscillations in the solid material
 tcycle = time in seconds of a cycle
 tlife = total expected shelf life in seconds to 80% capacity at 25C and 50% SOC
 T = battery temperature in degrees C
 Ta = battery absolute temperature in degrees K, Ta = T +273
 T_{fact} = coefficient of temperature in thermal aging model
 Tnom = reference battery temperature takes as 25C
 Tnabs = reference battery temperature K, Tnabs = Tnom + 273
 U0 = an activation energy for bond breaking
 Vmax = maximum open circuit voltage at full charge and temperature T=25
 Vnom = nominal open circuit voltage at SOC = 0.5 and T
 Voc = the open circuit voltage of the battery at a given SOC

References:

1. Ning, G; White, RE; Popov, BN , “A generalized cycle life model of rechargeable Li-ion batteries “, J. Electrochimica Acta 51 (10): 2012-2022, 1 Feb 2006.
2. M. Dubarry, V Svoboda, R Hwu, B.Y. Liaw, “Capacity Loss in Rechargeable Lithium Cells DURING Life Cycle Testing: The Importance of Determining State-of-Charge”, J. Power Sources 174, 1121-1125, 2007.
3. Ning, G and Popov, BN, “Cycle Life Modeling of Lithium Ion Batteries”, J. Electrochemical Soc. 151 (10) A1584-A1591, 2004.
4. A123 Systems, Inc, Gozdz et. Al., US Patent US7,387,851 B2, “Self-Organizing Battery Structure with Electrode Particles that Exert a Repelling Force on the Opposite Electrode”, 17 June 2008.
5. Unnewehr, L. E. and Nasar, S. A., Electric Vehicle Technology, John Wiley, pp. 81-91, 1982)
6. Rosenkrantz, C. (of Johnson Controls/Varta), “Plug In Hybrid Batteries”, workshop presentation p. 14, EVS20: The 20th International Electric Vehicle Symposium and Exhibition, 15 Nov. 2003
7. ThermoAnalytics, HEVsim Technical Manual, chapter “Battery Modeling”, 2008.

8. Marano V, Onori S, Guezennec Y and Rizzoni G, "Lithium -Ion Battery Life Estimation for Plug-In Hybrid Electric Vehicles", Vehicle Power and Propulsion Conference 09, paper TS04B-4, 2009.
9. Zhurkov S.N. (1965) "Kinetic Concept of Strength of Solids". *Int. J. Fract. Mech.* 1. 311–323.
10. A123Systems web site, data sheet MD100001-02 for high power lithium ion battery cell ANR26650M1A, www.a123systems.com, 2009.
11. Peterson S., Apt J., and Whitacre, J, "Lithium Ion Battery Cell Degradation Resulting from Realistic Vehicle and Vehicle- to Grid Utilization", *J. Pwr Sources* 195 (2010), 2385-2392, 6 Oct 2009.
12. Liaw, BY, Jungst RG, Nagasubramanian G, Case HL, and Doughty DH, "Modeling Capacity Fade in LithiumIon Cells", *J. Power Sources* 140 , 157-161, 2005.
13. Smith, K., Markel, T, and Pesaran, A., "PHEV Battery Trade-Off Study and Standby Thermal Control", 26th Internatl. Batery Seminar and Exhibit, Ft. Lauderdale, Florida, 16-19 March 2009, NREL/PR-540-45048.

This work was sponsored by the United States Government under Air Force contract FA8721-05-C-0002. Opinions, interpretations, conclusions, and recommendations are those of the author and not necessarily endorsed by the United States Government.